

PALEONTOLOGY

Shifts in food webs and niche stability shaped survivorship and extinction at the end-Cretaceous

Jorge García-Girón^{1,2,*}, Alfio Alessandro Chiarenza^{3†}, Janne Alahuhta¹, David G. DeMar Jr.^{4,5}, Jani Heino¹, Philip D. Mannion⁶, Thomas E. Williamson⁷, Gregory P. Wilson Mantilla⁴, Stephen L. Brusatte⁸

It has long been debated why groups such as non-avian dinosaurs became extinct whereas mammals and other lineages survived the Cretaceous/Paleogene mass extinction 66 million years ago. We used Markov networks, ecological niche partitioning, and Earth System models to reconstruct North American food webs and simulate ecospace occupancy before and after the extinction event. We find a shift in latest Cretaceous dinosaur faunas, as medium-sized species counterbalanced a loss of megaherbivores, but dinosaur niches were otherwise stable and static, potentially contributing to their demise. Smaller vertebrates, including mammals, followed a consistent trajectory of increasing trophic impact and relaxation of niche limits beginning in the latest Cretaceous and continuing after the mass extinction. Mammals did not simply proliferate after the extinction event; rather, their earlier ecological diversification might have helped them survive.

INTRODUCTION

Sixty-six million years (Ma) ago, one of the largest and most transformative cataclysms of the Phanerozoic occurred, when a ~10-km-wide extraterrestrial bolide struck the Yucatán Peninsula, in the Gulf of Mexico (1–4). This impact caused a panoply of ecological and environmental catastrophes, including tsunamis and wildfires, as well as global darkness (i.e., an “impact winter”) due to the injection of sunlight-blocking debris and climate-forcing gases into the atmosphere (1, 5, 6). These upheavals destabilized all trophic levels and triggered severe extinctions that spread devastation worldwide (2). In terrestrial environments, all non-avian dinosaurs, “archaic” birds, and pterosaurs vanished following the impact (7–9), while other groups, such as mammals (10, 11) and squamates (12), suffered considerable losses. On the other hand, groups such as freshwater salamanders, turtles, and crocodylians seemingly survived nearly unscathed (13). In the aftermath of this Cretaceous/Paleogene (K/Pg) mass extinction, surviving lineages recovered relatively rapidly (13–16), accompanied by concomitant ecospace shifts that favored their expansion into vacated niches and large-scale explosive radiations in placental mammals (17, 18), neornithine birds (8, 19), and squamates (20), laying the foundations for the diverse range of faunas that we share the planet with today.

It is widely postulated that the extinction of the non-avian dinosaurs resulted in empty niches and novel ecological opportunities for surviving organisms. This paradigm is based almost exclusively

on taxonomic (11, 21), morphological (10, 22), and phylogenetic (14, 23) evidence. Mass extinctions, however, act on the structure and function of ecosystems. Much less understood is how the ecology of dinosaurs, mammals, and other terrestrial animals changed in the lead-up to and aftermath of the extinction event. Focusing on functional and trophic ecology, rather than on the classic trends in biostratigraphic ranges (24), can help disentangle the potential ecological drivers of survivorship and recovery. Understanding the ecological dynamics of the latest Cretaceous faunal components is central to answering two long-standing questions. First, were non-avian dinosaurs in long-term decline before their end-Cretaceous demise (9, 25–31)? Second, why were some members of the terrestrial and freshwater biota (e.g., mammals, lizards, neornithine birds, and crocodylians) able to survive the mass extinction but not others?

These questions can be addressed by modeling long-term patterns in food webs (31, 32) and ecospace occupancy dynamics (i.e., the multidimensional combination of paleoenvironmental conditions under which species developed) (29, 33). Direct fossil evidence of trophic interactions is still limited (32, 34), but methodological advances in network theory (35) and ecological niche partitioning (36) might hold the key to long-standing questions about food web stability and the functional roles of species in ancient ecosystems, both of which are at the core of modern evolutionary and ecological research (34, 37–39). Although the application of these emerging approaches is not yet commonplace in paleontology, a few studies have demonstrated that they are ideal tools for revealing species habitat distributions in deep time (6, 29, 33, 40) and the tempo and mode of ecological reorganization after mass extinctions (37–39).

Here, we quantify the magnitude of ecological change before and after the K/Pg boundary, from the Campanian stage of the Late Cretaceous to the Danian stage of the early Paleogene (83.6 to 61.6 Ma ago). Our analyses are based on a spatiotemporally and taxonomically standardized presence-only dataset (Fig. 1A), comprising more than 1600 fossil occurrences representing more than 470 genera of cartilaginous and bony fish, salamanders, frogs,

Copyright © 2022
The Authors, some
rights reserved;
exclusive licensee
American Association
for the Advancement
of Science. No claim to
original U.S. Government
Works. Distributed
under a Creative
Commons Attribution
NonCommercial
License 4.0 (CC BY-NC).

¹Geography Research Unit, University of Oulu, PO Box 3000, FI-90014 Oulu, Finland. ²Department of Biodiversity and Environmental Management, University of León, Campus de Vegazana, 24007 León, Spain. ³Departamento de Ecología e Biología Animal, Grupo de Ecología Animal, Centro de Investigación Mariña, Universidade de Vigo, 36310 Vigo, Spain. ⁴Department of Biology, University of Washington and the Burke Museum of Natural History and Culture, Seattle, WA 98105, USA. ⁵Department of Paleobiology, National Museum of Natural History, Smithsonian Institution, Washington, DC 20560, USA. ⁶Department of Earth Sciences, University College London, Gower Street, WC1E 6BT London, UK. ⁷New Mexico Museum of Natural History and Science, Albuquerque, NM 87104, USA. ⁸School of GeoSciences, Grant Institute, University of Edinburgh, James Hutton Road, EH9 3FE Edinburgh, UK.

†These authors contributed equally to this work.

*Corresponding author. Email: jogarg@unileon.es

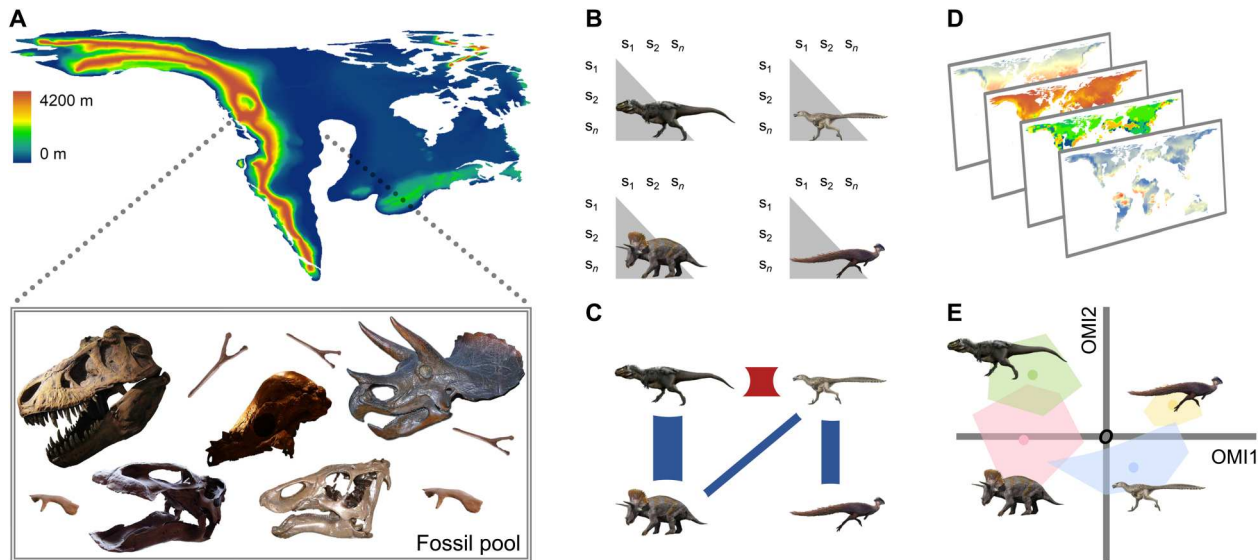


Fig. 1. Graphical scheme synthesizing the essential statistical routines used to reconstruct food web dynamics and quantify ecological niche partitioning in a set of hypothetical Maastrichtian (72.1 to 66.0 Ma ago) dinosaur communities across the ancient landscape of Laramidia. Briefly, (A) our dataset represents the record of North American tetrapod faunas, in which taxa were assigned to different trophic guilds using three ecological parameters (broad habitat-use types, body size, and feeding habits). We then built on (B) empirical spatial covariations to explore a map of dependencies between the residual signals of the Sørensen dissimilarities (i.e., $n \times n$ β -diversity matrices, n being the number of fossil localities s) without any a priori network structure (35, 99). (C) Conditional dependencies using partial correlation networks were estimated from the variance-covariance and precision matrices, and the overall importance of every trophic group on the food web architecture was inferred using the weighted degrees (50) and eigenvector centrality scores (51). Then, (D) we used a combination of state-of-the-art Earth System models (44–46) to create the paleoclimatic, land surface, and paleogeographical envelopes, and (E) ran the outlying mean index (OMI) approach (47) to obtain the marginality of species distributions (i.e., the Euclidean distances between the position of each group's species center of gravity, the colored points within each polygon, and the average paleo-environmental conditions O) and the realized species niche breadth (i.e., the corresponding polygon extent or the range of habitat conditions used by species). In this example, (C) partial correlation networks showed strong interactions between herbivorous and faunivorous dinosaurian guilds (34). (E) Giant theropods and their largest prey used relatively similar habitat conditions, although megaherbivores occupied a larger part of the available niche as a result of their potentially more cosmopolitan distribution in North America (133). Silhouettes and pictures were obtained from Wikimedia Commons (see Acknowledgments).

albanerpetontids, lizards, snakes, champsosaurs, turtles, crocodylians, dinosaurs (including birds), and mammals (e.g., table S1) across the best sampled region representing this interval (9), the Western Interior of North America [sensu Gardner and DeMar (41)]. This region includes the highly fossiliferous western subcontinent, Laramidia, which, during much of the Late Cretaceous, was separated from its eastern counterpart, Appalachia, by an epicontinental seaway stretching from present-day Alaska to Mexico. Using a spatially explicit Markov network approach (Fig. 1, B and C) (42, 43) and state-of-the-art Earth System models (Fig. 1D) (44–46), in combination with multivariate niche-modeling techniques (Fig. 1E)

(47), we simulate how inferred trophic dynamics and niche occupancy patterns shaped the trajectories of North American continental ecosystems across the latest Cretaceous and during the recovery from the mass extinction. By doing so, we explicitly test whether (i) shifts in food web architecture underwent major restructuring before and after the K/Pg extinction, including whether some trophic guilds were more prone to these shifts than others; and (ii) any of these changes were associated with fluctuations in the realized niche space, helping to explain why some groups survived and others went extinct across the K/Pg boundary.

RESULTS

Trophic network structure before and after the K/Pg mass extinction

Markov networks for Campanian (83.6 to 72.1 Ma ago) and Maastrichtian (72.1 to 66.0 Ma ago) food webs (Fig. 2) are composed of 43 and 34 undirected edges, respectively, out of 105 possible edges and 15 nodes, whereas those for the early Paleogene (66.0 to 61.6 Ma ago) have 13 nodes and are defined by 33 undirected edges (Fig. 2 and Table 1). Most non-null partial correlations during the K/Pg interval are positive (figs. S1 and S2). In this study, nodes represent different trophic guilds according to the ecology, body size, and habitat preferences of taxa (34, 37, 48, 49), and links (i.e., edges) represent the empirical dependencies between β -diversities of certain paleocommunity types (see Materials and Methods).

Table 1. The structure of the empirical trophic networks in North American ecosystems before and after the K/Pg extinction event. "Maximum" and "mean" are the maximum and mean values of the non-null partial correlation coefficients.

	Campanian	Maastrichtian	Danian
Undirected edges	43	34	33
Overall network connectance	0.41	0.32	0.42
Maximum	0.37	0.53	0.35
Mean	0.12	0.10	0.15
Centrality score	0.79	0.65	0.85

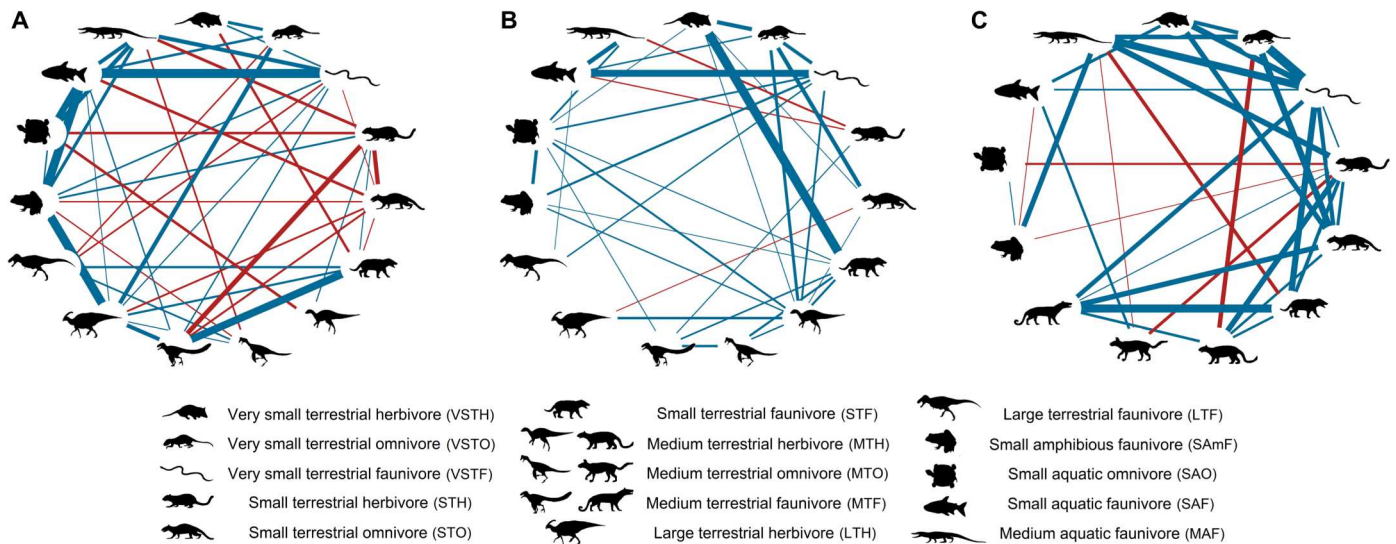


Fig. 2. Partial correlation networks before and after the end-Cretaceous mass extinction. Nodes represent the trophic guilds that constitute the food webs of the latest Cretaceous [(A) Campanian and (B) Maastrichtian] and early Paleogene [(C) Danian]. Line thickness is scaled to the linkage strength, and colors indicate positive (blue) or negative (red) partial correlation coefficients. Silhouettes were obtained from <http://phylopic.org/> (see Acknowledgments).

We recovered changes in interaction network topologies, connectance, and the number of guild interactions during the latest Cretaceous and into the Paleogene (Fig. 2), with Maastrichtian food webs showing lower overall connectance and eigenvector centrality values relative to both the Campanian and Danian (Table 1). Specifically, although the structuring role of large carnivorous theropods was mostly unchanged before their extinction, our analysis supports a progressive Campanian-to-Maastrichtian decline in the trophic impact (i.e., the influence that a trophic group has on the interactions among the remaining guilds) of large-bodied, bulk-feeding, herbivorous ornithischians (Figs. 2 and 3). This is shown by our measures of weighted degrees [i.e., the total sum of partial correlations between a given node and the other nodes that are directly connected to this group (50); Fig. 2] and centrality scores [i.e., the direct and indirect influence of each trophic group on the entire food web (51); Fig. 3]. Medium-sized herbivorous and omnivorous dinosaurs had a stronger influence on Maastrichtian food webs, whereas the trophic impact of medium-sized faunivorous theropods

was almost twice as high in the Campanian than in the Maastrichtian (Figs. 2 and 3).

The trophic impact of most very-small-to-small (≤ 10 kg) terrestrial vertebrates, including mammals, increased from the Campanian to the Maastrichtian and remained high and stable in the Danian, in terms of both weighted degrees and centrality scores (Fig. 3). Unlike the pattern of decreased trophic structuring for most amphibious (e.g., lissamphibians) and aquatic animals in continental food webs, their larger faunivorous counterparts, such as crocodylians and champsosaurs, increased their potential trophic impact after the end-Cretaceous mass extinction (Figs. 2 and 3).

These trophic patterns are robust to sensitivity analyses, including whether biases related to ecologically mediated species distributions [sensu Dormann *et al.* (52)] and systematic sampling biases could alter our findings in terms of weighted degrees and eigenvector centrality values (figs. S3 and S4, *ibid.*). We show that these trophic parameters are not correlated with fluctuations in observed species richness (paired samples *t*-tests, $P = 0.56$ to 0.89 ; fig. S5), nor

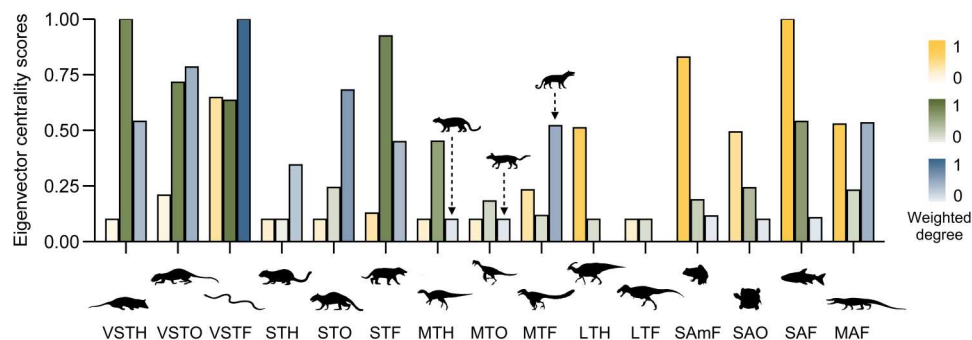


Fig. 3. Properties of the inferred food webs before and after the end-Cretaceous mass extinction. This figure represents the eigenvector centrality scores and weighted degrees for each trophic guild in the food webs of the latest Cretaceous (Campanian: yellow; Maastrichtian: green) and early Paleogene (Danian: blue). The eigenvector centrality quantifies the standardized importance of each node for the overall connection of the interaction network (51), and the weighted degree is the sum of partial correlations between a given node and the other nodes that are directly connected to this trophic group (50). Silhouettes and abbreviations of representative animals follow Fig. 2 and were obtained from <http://phylopic.org/> (see Acknowledgments).

do they suffer from weaknesses associated with spatial autocorrelation (fig. S6). These patterns also remain after a random resampling of both fossil localities (paired samples *t*-tests, $P = 0.23$ to 0.81 ; fig. S7) and taxa (paired samples *t*-tests, $P = 0.08$ to 0.94 ; fig. S8), providing further support for the robustness of our interpretations. These results are also compatible with an undersampling of small-sized taxa in both Campanian (53) and Maastrichtian (54) faunas.

Ecospace dynamics underlying observed trophic shifts

The shift in trophic structure across dinosaur-dominated guilds from the Campanian to Maastrichtian, especially those occupied by large herbivores (see above), was not accompanied by concomitant changes in ecospace occupancy patterns (Fig. 4), whether based on species realized niche position [i.e., the marginality of species habitat distributions, *sensu* Dolédec *et al.* (47)] or breadth [i.e., the range of habitat conditions occupied by each species, *sensu* Dolédec *et al.* (47)]. These two ecospace measures are robust to subsampling approaches (fig. S9). The lack of statistically significant long-term changes in niche occupancy was also shared by most amphibious and aquatic vertebrate communities (Fig. 4). In addition, whereas very small terrestrial herbivores adopted a more specialist strategy and were less widespread across the paleoenvironmental gradient after the K/Pg boundary, the remaining very-small-to-small-sized terrestrial species—including most mammals—followed a consistent trajectory, increasing their habitat distributions and realized niche breadth throughout the Late Cretaceous and into the early Paleogene (Fig. 4 and tables S2 and S3). The mean

expansion of species habitat distributions preceding the K/Pg boundary was significantly higher for these very-small-to-small terrestrial faunas than that experienced by non-avian dinosaurs (Kruskal-Wallis, $P < 0.01$), and we document a similarly steady rise in ecospace occupancy patterns for mammalian faunas alone (fig. S10 and table S4).

DISCUSSION

Food web dynamics contributed to extinction selectivity during the K/Pg mass extinction

Our results suggest that trophic restructuring in the latest Cretaceous played a role in both the tempo and mode of extinction across the K/Pg boundary, as well as the subsequent recovery of ecosystems. The latest Cretaceous decrease in trophic impact of large herbivorous dinosaurs does not correspond with instability in their realized niches, which argues against a long-term ecological “decline” in these plant eaters (9, 29, 55). Rather, the decreasing impact of large herbivores was paralleled by an inverse trend of increasing trophic relevance for medium-sized herbivorous and omnivorous dinosaurs. These ecological changes concur with a marked latest Cretaceous decline in morphological disparity in large-bodied ceratopsid and hadrosauroid ornithischian dinosaurs in western North America (9). We interpret these patterns as evidence of large-scale trophic replacement of the largest herbivorous dinosaurs by their smaller counterparts in North American ecosystems. It has been suggested that the ecological reorganization of the megaherbivore guild led to more unstable food webs in the Maastrichtian (37),

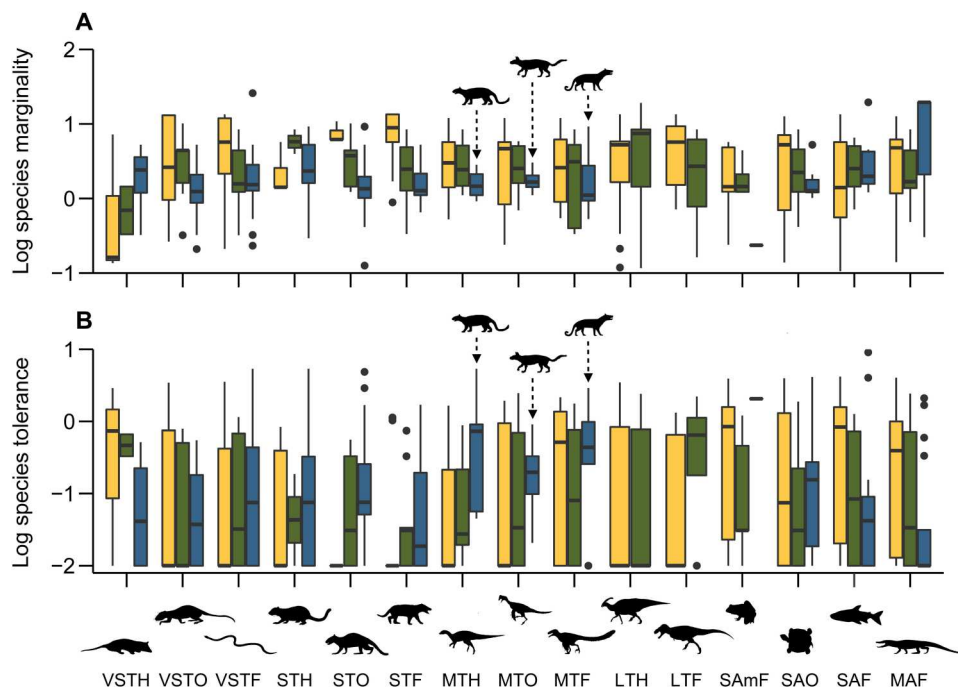


Fig. 4. Niche occupancy dynamics before and after the end-Cretaceous mass extinction. Boxplots show the distribution of the log-scaled species marginality (A) and tolerance (B) for each trophic group across the latest Cretaceous (Campanian: yellow; Maastrichtian: green) and early Paleogene (Danian: blue). The lower the species marginality (i.e., niche position), the less different its habitat preferences are from the average paleoenvironmental conditions. The higher the species tolerance (i.e., niche breadth), the more widely a species occurs across broad paleoenvironmental ranges. Boxplot bold lines indicate the median, whereas the boxes and whiskers are the interquartile range (IQR) and the maximum and minimum up to $1.5 \times$ IQR, respectively. Silhouettes and abbreviations of representative animals follow Fig. 2 and were obtained from <http://phylopic.org/> (see Acknowledgments).

with cascading effects on predators and scavengers (56, 57), as has been documented in extant ecosystems of the African savanna (58) and elsewhere (59). The lower connectance and centrality score values (Table 1) for Maastrichtian, compared to Campanian, food webs agree with this observation, suggesting that medium-sized dinosaur-dominated guilds did not entirely compensate for the loss of trophic resources from the largest bulk-feeding ornithischians. Instead, these roles were partially filled by much smaller non-dinosaurian vertebrates, such as multituberculate and metatherian mammals (data S2 and S3).

Despite a decrease in trophic impact, the lack of any meaningful long-term change in species realized niche position or breadth across the megaherbivores (or any other non-avian dinosaur guild) is instead an indication of relative stability in ecospace occupancy, which can be decoupled from food web dynamics. An absence of long-term niche breadth decline in dinosaurs (29) is also supported by their highly diverse anatomies and functional abilities until the end of the Cretaceous (60–62), which would have promoted dietary and habitat niche partitioning between sympatric taxa (57, 63, 64).

Ecological evidence (29, 65), including the multidimensional niches presented here, paints a nuanced picture of the final 18 Ma of non-avian dinosaur existence. Despite substantial food web restructuring before their extinction, non-avian dinosaurs seem to have been characterized by largely stable and mostly static ecological niches during the Campanian and Maastrichtian, likely due to a large spectrum of already inhabited ecologies and morphotypes (25, 29, 55, 60, 61). However, niche stability might have placed dinosaur-dominated guilds at a disadvantage in the event of an abrupt shutdown of the trophic network, such as that experienced at the K/Pg boundary (1). By contrast, the increase in trophic impact of smaller-sized, terrestrial taxa—including mammals—during the Maastrichtian might have helped prepare these more highly plastic guilds for differentially greater survivorship during the K/Pg mass extinction, most likely because increased numbers of trophic interactions and relaxation of niche limits may have buffered against the effects of the extinction cascades that followed the end-Cretaceous bolide impact (1, 6, 16). This, in part, might help explain why mammals were able to make it through the extinction event, despite high species losses (11, 66), whereas non-avian dinosaurs were not.

Transient selectivity against large-bodied taxa, particularly strictly faunivorous and herbivorous species, cannot alone explain the eradication of small-bodied archaic birds (e.g., enantiornithines) and non-avian dinosaurs (e.g., alvarezsaurids and microraptorine dromaeosaurids), some of which were around the size of many mammals that did survive the mass extinction (10, 12, 60, 67–69). High abundances of individuals in their ecosystems, omnivorous and seed-eating diets (60, 69), cathemeral habits (15), more rapid somatic and sexual development (70), and behavioral plasticity (71) might have enabled certain smaller taxa, such as non-marine squamates, crown birds, and mammals, to survive the effects of the Chicxulub impact (Fig. 4). As such, their greater pre-impact niche plasticity might have made them less susceptible to major environmental perturbations and more adaptive to new conditions.

Trophic and ecospace expansion of small terrestrial vertebrates before and after the K/Pg mass extinction

Paleontological discoveries have traditionally supported the longstanding “suppression hypothesis” that the end-Cretaceous mass

extinction triggered a prolific ecological release of the survivors in terms of ecomorphological diversity (10, 11, 15, 18, 21, 22). However, the view that Mesozoic mammals and crown group birds, living amidst non-avian dinosaurs, were ecologically depauperate and suppressed has been increasingly questioned (7, 8, 72–74). Our results show that the weighted degrees and centrality scores of very small herbivores and small faunivores were almost 10 times greater in the Maastrichtian than in the Campanian. This emphasizes that the latest Cretaceous was also a pivotal time for the trophic and ecological evolution of terrestrial non-dinosaurian vertebrates, as attested by the records of multituberculate, metatherian, and early-diverging eutherian mammals (18, 68, 72, 75), squamates (12, 20, 76), crocodyliforms (77), and enantiornithine and early-diverging ornithurine birds (7, 60).

Evidence of a meaningful pre-K/Pg shift in mammalian evolution and ecological diversification is supported by analyses of morphometric (10, 22, 72, 73) and molecular genomic (14, 23) data (although it should be noted that these studies do not commonly argue for major anatomical, body size, or ecological diversifications of modern placental groups until after the extinction event). These studies have noted congruent trends in the expansion of ecological boundaries during and after the Late Cretaceous [reviewed by Grossnickle *et al.* (18)]. It is interesting to note that similar patterns co-occur for most very-small-to-small-sized terrestrial vertebrates, with relaxation of their niche limits in the latest Cretaceous followed by concurrent higher weighted degrees and centrality scores in the trophic networks in the Paleogene.

Our results suggest that survivors took advantage of new ecological opportunities after the K/Pg boundary, expanding into new habitats during the first few million years of the Paleogene (Fig. 4). This opportunistic scenario might have occurred because these taxa exploited a range of niches previously occupied by the Maastrichtian victims (10, 15, 18, 73), and/or because the resources that were available for these vertebrates were relatively unaffected by the bolide impact (72). In comparison with omnivorous guilds, the structuring role of very small terrestrial herbivores and small faunivores was 50% less impactful in the earliest Paleogene than that of the Maastrichtian (Fig. 3). This supports the hypothesis that organisms with more generalized diets were less affected by the end-Cretaceous mass extinction (10), as suggested for opportunistic squamates (12, 20), crocodylians (78), and multituberculates (72).

Resilience of freshwater communities during the end-Cretaceous mass extinction event

We observe a shift in the trophic impact of most aquatic animals through the latest Cretaceous and into the Paleogene. Whereas most amphibious and aquatic animals showed a decreased structuring role in continental food webs, their faunivorous counterparts, such as crocodylians and champsosaurs, increased their trophic impact after the end-Cretaceous mass extinction (Figs. 2 and 3). The predominance of larger faunivorous taxa in these settings could indicate a healthier fluvio-lacustrine ecosystem, at least enough to warrant the survivorship and flourishing of taxa that were previously apex predators. Given the relatively low niche marginality values of small amphibious and aquatic faunivores and omnivores (Fig. 4), there is reason to believe that these animals were not so strongly affected by the sudden extinction event and its subsequent effects on survivors (79–82). The extinction of several taxa of freshwater sharks and rays indicates that the bolide impact

caused some degree of disruption at high trophic levels in these ecosystems at the very end of the Cretaceous (83). However, we document no meaningful changes in long-term trajectories in ecospace occupancy patterns for most of these amphibious and aquatic communities well before and after the K/Pg boundary (during the recovery phase).

Our findings quantitatively corroborate the notion that river and lake ecosystems were relatively resilient to the extinction event. For example, the fossil record shows that many lineages of teleost fish extended from the Cretaceous well into the Cenozoic (84–87), as did several aquatic and amphibious tetrapods that inhabited the fertile floodplains of North America, such as turtles (82), lissamphibians (13), and crocodylians (88). These floodplains and fluvio-lacustrine systems might have acted as ecological refugia against intense environmental perturbations caused by the bolide impact (89). This hypothesis is based on the purported high thermal inertia provided by inland waters. Also, these habitats might have acted as biotopic shelters via microhabitat heterogeneity for multiple animal groups, and because their food webs were more reliant on the resilient detritus cycle than on photosynthesizing plants (6, 80, 90).

Tempo and mode of North American non-marine ecosystem changes across the K/Pg

Our work adds a food web and ecological niche dimension to our understanding of the K/Pg mass extinction. Whether these findings are representative of a global reality must be tested in the future with fossil datasets beyond the Western Interior of North America, and baseline comparisons among different continents are worth additional study. Nevertheless, our results confirm that there was a decline in the large-bodied, preeminent herbivorous ornithischian dinosaur guild from the Campanian to the Maastrichtian, at least in North America, which probably made terminal Cretaceous food webs more fragile in the face of the bolide impact (9, 37). However, claims for a gradual downturn across most non-avian dinosaurian lineages, causing major shifts in ecospace occupancy (26, 27, 31), are not supported by our findings, as dinosaurs experienced largely static and mostly stable niches during the Campanian-Maastrichtian interval, until the bolide impact. Smaller-sized, terrestrial tetrapods took advantage of new ecological opportunities in the aftermath of the Chicxulub impact, while most amphibious and aquatic faunas suffered relatively less marked trophic and ecospace dynamics. Critically, we demonstrate that very-small-to-small-sized Mesozoic vertebrates, including mammals (18, 68, 72, 75), squamates (12, 20), and crown group birds (7, 60), underwent major ecological restructuring that began by the Maastrichtian and before the bolide impact. Thus, these groups were not mere beneficiaries of vacated niches, but their earlier ecological diversification probably helped prime them for survivorship in the post-impact recovery. It was this interplay of ecology, extinction, and survivorship that ultimately laid the foundations for the characteristic terrestrial, lacustrine, and fluvial biotas of today.

MATERIALS AND METHODS

Fossil dataset

For this study, we compiled a presence-only fossil occurrence dataset for all terrestrial and fluvio-lacustrine vertebrate taxa from the Campanian-Danian of North America. We originally downloaded fossil and taxonomic occurrences detailing Upper

Cretaceous (Campanian-Maastrichtian) and early Paleogene (Danian) formations across North America from the Paleobiology Database (paleobiodb.org, accessed June 2020). These fossil occurrences were further edited until February 2022 and recently reviewed in the database by one of us (P.D.M.). To complement these occurrences (Fig. 1A), supplementary information (e.g., stratigraphic placement) from published sources and publicly available collections was integrated by several of us (A.A.C., D.G.D., P.D.M., T.E.W., G.P.W.M., and S.L.B.). Taxa with unclear genus identification were discarded [i.e., we did not incorporate “cryptic” diversity represented by taxonomically undiagnostic fossil remains, nor did we infer ghost lineages based on phylogenetic diversity (91, 92)], as were para-taxonomic taxa [e.g., trace remains and eggs (37, 65)]. If questionable ages and stratigraphic incongruencies emerged, occurrences were either revised following the most recent stratigraphic models [e.g., (93, 94)] or excluded. Overall, our dataset is a taxonomically and stratigraphically up-to-date record of North American vertebrate faunas and therefore incorporates latest Cretaceous and early Paleogene fossils discovered over the past few years, with more than 470 taxa represented by ~1600 occurrences (data S2 and S3).

Synthesizing food webs across the K/Pg extinction event Trophic structure and delineations

We assigned taxa to guilds based on habitat, body size, and feeding habits (34, 37, 48, 49). Broad habitat-use types were subdivided into two major categories: aquatic and terrestrial. For those taxa that were likely in and out of the water through their life history (e.g., lissamphibians), we included an additional habitat division, i.e., amphibious (table S1). Body size is perhaps the single most important and meaningful trait for animals, as it ultimately affects multiple aspects of their biology, including mechanical constraints, metabolic rates, food resource use, population size, lifestyle strategies, and geographical ranges, determined by physiology, locomotion, reproduction success, and survival (95, 96). On the other hand, trophic habits refer to the diet and food processing strategies of an animal, and it generally includes three primary categories, i.e., herbivores, faunivores, and omnivores. In the present study, we assigned body size (i.e., large, medium, small, and very small) and feeding habit (i.e., herbivore, faunivore, and omnivore) divisions integrating data from several comprehensive datasets [e.g., (10, 34, 37, 73, 97, 98)]. Following Mitchell *et al.* (37), we assigned taxa to trophic guilds based on adult representatives, which allowed us to represent the complete potential dietary suite of members, thereby producing complex but realistic interaction networks (see table S1 for examples). Pragmatically, further subdividing animal groups into trophic guilds (e.g., carnivores versus insectivores, low browsers versus high browsers) might have compromised the parsimonious representation of conditional dependencies in Markov networks [see (42, 43) and (99) for details].

Model description

Ohlmann *et al.* (35) proposed a framework for inferring and plotting the strength of conditional (spatial) dependencies between pairs of trophic groups using a blockwise coordinate descent procedure for the least absolute shrinkage and selection operator (Lasso) regularization approach (100), i.e., the Graphical Lasso [GL; (42, 43)]. This method uses partial correlation networks to parsimoniously represent how different trophic groups interact in a food web, allowing the representation of the conditional dependencies among

multiple variables in these networks. In other words, the GL approach builds on empirical spatial covariations to explore a map of dependencies between β -diversities of trophic groups (35). Here, we computed pairwise β -diversities for multiple trophic groups as the Sørensen dissimilarity matrix (101) in the R package BAT (102). Numerically, this statistical routine calculates a partial correlation matrix that quantifies the degree of relationship (weighted coefficients) between pairs of variables conditional to the other variables (here, an $n \times n$ β -diversity matrix, n being the number of fossil-bearing localities s ; Fig. 1B). To do this, the GL routine initiates by producing an empirical variance-covariance matrix \mathbf{S} , which is then inverted to compute a precision matrix \mathbf{P} ($\mathbf{P} = \mathbf{S}^{-1}$). Compared to other mathematical methods that estimate interaction coefficients, this approach uses a penalty term in the likelihood (modulated by the λ coefficient) to control the sparsity of the precision matrix \mathbf{P} [see the study of Friedman *et al.* (42) for details]. Following Foygel and Drton (103), we selected the optimal number of the λ coefficient based on the extended Bayesian information criteria. The partial correlation matrix was then calculated from the precision matrix \mathbf{P} with the R package qgraph (104) as follows

$$\text{cor}(x_i, x_j | x_{\setminus\{i,j\}}) = -\frac{P_{ij}}{P_{i,i}P_{j,j}}$$

where $\text{cor}(x_i, x_j | x_{\setminus\{i,j\}})$ is the partial correlation between the components i and j of a random variable X given all the other components, and $P_{i,j}$, $P_{i,i}$, and $P_{j,j}$ are the elements of the precision matrix \mathbf{P} . Because the precision matrix \mathbf{P} was inverted with a penalty term modulated by λ , the partial correlation matrix $\text{cor}(x_i, x_j | x_{\setminus\{i,j\}})$ was also sparse (42, 43). Hence, the final product of the GL is a Markov network portrayed by an adjacency matrix with weighted coefficients for the trophic guilds (105).

We repeated the models independently for each time interval (Campanian, Maastrichtian, and Danian), yielding three different food webs or ecological networks (Fig. 1C). Following Ohlmann *et al.* (35), García-Girón *et al.* (99), and Lansac-Tôha *et al.* (105), the overall importance of every trophic group (each node) on network structures was inferred through a combination of the weighted degrees [the total sum of partial correlations between a given node and the other nodes that are directly connected to this group (50)] and the eigenvector centrality values [the direct and indirect influence of each trophic group on the entire food web (51)]. In this context, the higher the sum of the weighted degrees or the more inflated centrality scores, the greater the conditional dependencies of a trophic group with the β -diversity of the remaining guilds (50). In other words, the more connected a trophic group is, the stronger influences it makes on the interactions among the remaining guilds, although these inferred conditional dependencies do not necessarily imply causality (35).

Accounting for competing biases in our modeling results

The GL approach is expected to be sensitive to the effect of missing environmental covariates and the heterogeneous distribution of sampling efforts (35). In the words of Dormann *et al.* (52) (p. 1008), when disentangling species interactions from other factors that can affect co-occurrence at the macroscale: "species (or groups of species) with similar habitat requirements will appear to interact positively, whereas species (or groups of species) that have contrasting requirements will appear to interact

negatively." Specifically, the inference of the conditional dependencies under GL would be jeopardized if, as is often the case in ecology and paleoecology, species share similar habitat preferences (52), or if the fossil record and animal distributions are compromised by incompleteness and bias (106) or are spatially autocorrelated (107), respectively. Under these circumstances, skepticism over the value of statistical inference is justified and was a pivotal issue to verify in our model outputs.

To correct for these confounding artifacts, we first adapted the step-by-step approach of Lloyd (108) to assess both the influence of potentially shared responses to paleoenvironmental conditions (here, paleoclimate, land surfaces, and paleogeography; see below) and the unequal distribution of sampling effort [here, the number of discrete tetrapod-bearing collections (109–112)] on the β -diversities that constitute that backbone of the GL routine. In our case, we evaluated the relationships between β -diversities of each trophic guild and a subset of orthogonal eigenvectors from factorial analysis of mixed data (PCAMIX) through linear regressions, accompanied by Akaike's information criteria to fit the best linear versus quadratic model. All quantitative explanatory variables (i.e., paleoclimatic, land surface, and paleogeographical envelopes, as well as sampling proxy values) were scaled between 0 and 1, and we retained as many PCAMIX eigenvectors as required to maximize the fit between response and explanatory matrices (113). Predicted spatial variations for each trophic guild and the residual unexplained signals (scaled) were produced and subsequently used as a corrected estimate of Sørensen dissimilarities for computing the empirical variance-covariance matrix \mathbf{S} and its associated precision matrix \mathbf{P} under the GL routine (114).

Because metrics of β -diversity ambiguously capture the spatial turnover when compared across fossil localities with different number of species (115), we partitioned the Sørensen index into its true species replacement component (116) and checked whether the structure of the empirical food webs was partly driven by fluctuations in observed species richness. We also ran Mantel correlograms to (i) account for the spatial structures in detail and (ii) test whether pairwise β -diversities of each individual trophic guild were spatially autocorrelated. Here, distance classes were determined by Sturge's rule (101), and P values were based on 199 permutations with Holm correction for multiple testing (117). Following García-Girón *et al.* (99), we lastly assessed the uncertainty of the empirical Markov networks through a set of sensitivity analyses based on a random resampling of the fossil localities and taxa for 99 iterations (118, 119). We then compared the matches between the eigenvector centrality values from the previous routines and the entire dataset with paired samples t -tests (120). This combination of routines allows our results to be evaluated as robust even in the light of heterogeneous biases that are so pervasive in the vertebrate fossil record and spatial and habitat-preference dependencies that can obfuscate the statistical significance of such paleoecologically relevant findings.

GCM-derived paleoclimates, land surfaces, and paleogeographical DEMs

Paleoclimatic and land surface model outputs used in this study come from the fully coupled AOGCM HadCM3L version 4.5 from the BRIDGE Group (www.bridge.bris.ac.uk/resources/simulations) and, more specifically, the HadCM3BL-M2-1aE version of the model. Variables include near-surface (1.5 m)

mean annual temperature (°C), near-surface (1.5 m) annual temperature SD (°C), annual average precipitation (mm), annual precipitation SD (mm), net primary productivity ($\text{g C m}^{-2} \text{ year}^{-1}$), and plant functional types (i.e., from broadleaf and needleleaf trees to C3-type and C4-type groundcover) at $2.75^\circ \times 3.25^\circ$ spatial resolution. The simulations and settings of the terminal Cretaceous and early Paleogene models used here are described in full by Lunt *et al.* (44), Valdes *et al.* (45), and Farnsworth *et al.* (121), and implications of these general circulation modeling (GCM) constraints are discussed by Chiarenza *et al.* (6, 29, 65, 122), Dunne *et al.* (123), and Waterson *et al.* (124). Briefly, all model simulations underwent the same spin-up procedure and were run for a total of 1422 years reaching quasi-surface equilibrium, with the same initial conditions and boundary conditions (44), with the exception of solar constant (table S5) and paleogeography. Solar luminosity was calculated for each time interval, and we used a modern-day orbital configuration and an atmospheric CO₂ concentration of 1120 ppmv, which is within the range of uncertainty from that of Foster *et al.* (125) for these time intervals. Variables used in our study were an annual average of the last 30 years of these simulations. Temporal fluctuations, as well as regional and large-scale circulations, including associated energy and momentum fluxes, are also resolved in the models (44). Given the uncertainty of the data, these models accurately reproduce modern-day climates of most terrestrial biomes (45). HadCM3L has contributed to Coupled Model Intercomparison Project experiments and demonstrated skill for an array of Mesozoic paleobiogeographical studies (6, 29, 65, 123). However, there is still a high degree of uncertainty in pCO₂ proxies during the Phanerozoic and paleoclimatic reconstructions in general (123–125), and ongoing work will continue to constrain these data and their impact on modeling niche occupancy dynamics of ancient faunas.

The paleogeographies used for this study are those of Scotese and Wright (46), originally created as a paleo-digital elevation model (DEM) on a $1^\circ \times 1^\circ$ grid and upscaled to the HadCM3L Earth System model resolution ($2.75^\circ \times 3.25^\circ$). This means that topographic and bathymetric information was broadly conserved as it was resolved at a lower spatial resolution (6, 34, 65). These 117 maps have provided a global atlas for regional-scale paleogeographical interpretations of the last 540 million years, including changing distributions of world's oceans and continents. Additional information is available at www.earthbyte.org/.

Ecological niche partitioning

Species niches cannot be calculated directly from an n -dimensional hypervolume [sensu Hutchinson (126)], but multivariate ordination techniques are the best-suited proxies to evaluate the realized ecological niche of each taxon while explicitly accounting for species-environment relationships (36). Here, we used the outlying mean index (OMI) framework (47) to obtain measures of niche position and niche breadth (Fig. 1, D and E). Compared to other ordination methods, the OMI routine is robust to multicollinearity among predictors and describes species responses irrespective of whether they are linear or unimodal, giving equal weight to species-poor and species-rich fossil localities (47). Pragmatically, the OMI approach seeks for combinations of paleoenvironmental mechanisms (here, scaled paleoclimatic, land surface, and paleogeographical envelopes) that maximize the marginality of species habitat distributions, i.e., the squared Euclidean distances between

the mean habitat conditions used by a species (species center of gravity) and the average paleoenvironmental conditions of each time interval. High marginality values suggest that species are found under marginal or atypical habitat conditions, whereas low scores indicate that a species is more or less uniformly distributed (ubiquitous) across the entire paleoenvironmental gradient. The niche axis is also decomposed in terms of species tolerance, which measures the range of habitat conditions used by a species and can be considered as a proxy for the realized habitat niche breadth (127). Species showing high values of tolerance are distributed across broad paleoenvironmental gradients and have large niches, whereas low tolerance values imply that species occur only across a limited range of habitat conditions and have small niches (127–129). Independently of the time bin (Campanian, Maastrichtian, and Danian) and using the R package *ade4* (130), we calculated both realized habitat niche position and niche breadth values for all taxa, including very rare ones. We further ran Kruskal-Wallis routines and associated multiple comparisons (131) to test for a measurable niche occupancy shift across faunal groups during the K/Pg extinction event. Last, the same sensitivity test as applied under the GL approach was used to assess the impact of various issues related to fossil preservation and animal distribution biases that might affect estimates of ecospace occupancy dynamics (see above for details). All modeling exercises were run in the R environment (132).

Supplementary Materials

This PDF file includes:

Figs. S1 to S10
Tables S1 to S5

Other Supplementary Material for this

manuscript includes the following:

Data S1 to S3

REFERENCES AND NOTES

1. L. W. Alvarez, W. Alvarez, F. Asaro, H. V. Michel, Extraterrestrial cause for the Cretaceous-Tertiary extinction. *Science* **208**, 1095–1108 (1980).
2. P. Schulte, L. Alegret, I. Arenillas, J. A. Arz, P. J. Barton, P. R. Bown, T. J. Bralower, G. L. Christeson, P. Claeys, C. S. Cockell, G. S. Collins, A. Deutsch, T. J. Goldin, K. Goto, J. M. Grajales-Nishimura, R. A. F. Grieve, S. P. S. Gulick, K. R. Johnson, W. Kiessling, C. Koeberl, D. A. Kring, K. G. M. Leod, T. Matsui, J. Melosh, A. Montanari, J. V. Morgan, C. R. Neal, D. J. Nichols, R. D. Norris, E. Pierazzo, G. Ravizza, M. Rebolledo-Vieyra, W. U. Reimold, E. Robin, T. Salge, R. P. Speijer, A. R. Sweet, J. Urrutia-Fucugauchi, V. Vajda, M. T. Whalen, P. S. Willumsen, The Chicxulub asteroid impact and mass extinction at the Cretaceous-Paleogene boundary. *Science* **327**, 1214–1218 (2010).
3. P. R. Renne, A. L. Deino, F. J. Hilgen, K. F. Kuiper, D. F. Mark, W. S. Mitchell, L. E. Morgan, R. Mundil, J. Smit, Time scales of critical events around the Cretaceous-Paleogene boundary. *Science* **339**, 684–687 (2013).
4. P. M. Hull, A. Bornemann, D. E. Penman, M. J. Henehan, R. D. Norris, P. A. Wilson, P. Blum, L. Alegret, S. J. Batenburg, P. R. Bown, T. J. Bralower, C. Courneade, A. Deutsch, B. Donner, O. Friedrich, S. Jehle, H. Kim, D. Kroon, P. C. Lippert, D. Lorocho, I. Moebius, K. Moriya, D. J. Peppe, G. E. Ravizza, U. Röhl, J. D. Schueth, J. Sepúlveda, P. F. Sexton, E. C. Sibert, K. K. Śliwińska, R. E. Summons, E. Thomas, T. Westerhold, J. H. Whiteside, T. Yamaguchi, J. C. Zachos, On impact and volcanism across the Cretaceous-Paleogene boundary. *Science* **367**, 266–272 (2020).
5. D. A. Kring, The Chicxulub impact event and its environmental consequences at the Cretaceous-Tertiary boundary. *Palaeogeogr. Palaeoclimatol. Palaeoecol.* **255**, 4–21 (2007).
6. A. A. Chiarenza, A. Farnsworth, P. D. Mannion, D. J. Lunt, P. J. Valdes, J. V. Morgan, P. A. Allison, Asteroid impact, not volcanism, caused the end-Cretaceous dinosaur extinction. *Proc. Natl. Acad. Sci. U.S.A.* **117**, 17084–17093 (2020).

7. N. R. Longrich, T. Tokaryk, D. J. Field, Mass extinction of birds at the Cretaceous–Paleogene (K–Pg) boundary. *Proc. Natl. Acad. Sci. U.S.A.* **108**, 15253–15257 (2011).
8. A. Feduccia, Avian extinction at the end of the Cretaceous: Assessing the magnitude and subsequent explosive radiation. *Cretac. Res.* **50**, 1–15 (2014).
9. S. L. Brusatte, R. J. Butler, P. M. Barrett, M. T. Carrano, D. C. Evans, G. T. Lloyd, P. D. Mannion, M. A. Norell, D. J. Peppé, P. Upchurch, T. E. Williamson, The extinction of the dinosaurs. *Biol. Rev.* **90**, 628–642 (2015).
10. G. P. Wilson, Mammals across the K/Pg boundary in northeastern Montana, U.S.A.: Dental morphology and body-size patterns reveal extinction selectivity and immigrant-fueled ecospace filling. *Paleobiology* **39**, 429–469 (2013).
11. N. R. Longrich, J. Scriberas, M. A. Wills, Severe extinction and rapid recovery of mammals across the Cretaceous–Paleogene boundary, and the effects of rarity on patterns of extinction and recovery. *J. Evol. Biol.* **29**, 1495–1512 (2016).
12. N. R. Longrich, B.-A. S. Bhullar, J. A. Gauthier, Mass extinction of lizards and snakes at the Cretaceous–Paleogene boundary. *Proc. Natl. Acad. Sci. U.S.A.* **109**, 21396–21401 (2012).
13. G. P. Wilson, D. G. DeMar Jr., G. Carter, Extinction and survival of salamander and salamander-like amphibians across the Cretaceous–Paleogene boundary in northeastern Montana, USA, in *Through the End of the Cretaceous in the Type Locality of the Hell Creek Formation in Montana and Adjacent Areas*, G. P. Wilson, W. A. Clemens, J. R. Horner, J. H. Hartman, Eds. (Geological Society of America, 2014), vol. 503.
14. T. J. D. Halliday, P. Upchurch, A. Goswami, Eutherians experienced elevated evolutionary rates in the immediate aftermath of the Cretaceous–Palaeogene mass extinction. *Proc. R. Soc. B: Biol. Sci.* **283**, 20153026 (2016).
15. R. Maor, T. Dayan, H. Ferguson-Gow, K. E. Jones, Temporal niche expansion in mammals from a nocturnal ancestor after dinosaur extinction. *Nat. Ecol. Evol.* **1**, 1889–1895 (2017).
16. T. R. Lyson, I. M. Miller, A. D. Bercovici, K. Weissenburger, A. J. Fuentes, W. C. Clyde, J. W. Hagadorn, M. J. Butrim, K. R. Johnson, R. F. Fleming, R. S. Barclay, S. A. McCracken, B. Lloyd, G. P. Wilson, D. W. Krause, S. G. B. Chester, Exceptional continental record of biotic recovery after the Cretaceous–Paleogene mass extinction. *Science* **366**, 977–983 (2019).
17. J. Alroy, The fossil record of North American mammals: Evidence for a Paleocene evolutionary radiation. *Syst. Biol.* **48**, 107–118 (1999).
18. D. M. Grossnickle, S. M. Smith, G. P. Wilson, Untangling the multiple ecological radiations of early mammals. *Trends Ecol. Evol.* **34**, 936–949 (2019).
19. R. O. Prum, J. S. Berv, A. Dornburg, D. J. Field, J. P. Townsend, E. M. Lemmon, A. R. Lemmon, A comprehensive phylogeny of birds (Aves) using targeted next-generation DNA sequencing. *Nature* **526**, 569–573 (2015).
20. M. C. Grundler, D. L. Rabosky, Rapid increase in snake dietary diversity and complexity following the end-Cretaceous mass extinction. *PLOS Biol.* **19**, e3001414 (2021).
21. T. W. Davies, M. A. Bell, A. Goswami, T. J. D. Halliday, Completeness of the eutherian mammal fossil record and implications for reconstructing mammal evolution through the Cretaceous/Paleogene mass extinction. *Paleobiology* **43**, 521–536 (2017).
22. T. J. D. Halliday, A. Goswami, Eutherian morphological disparity across the end-Cretaceous mass extinction. *Biol. J. Linn. Soc.* **118**, 152–168 (2016).
23. R. W. Meredith, J. E. Janečka, J. Gatesy, O. A. Ryder, C. A. Fisher, E. C. Teeling, A. Goodbla, E. Izirić, T. L. L. Simão, T.-J. Stadler, D. L. Rabosky, R. L. Honeycutt, J. J. Flynn, C. M. Ingram, C. Steiner, T. L. Williams, T. J. Robinson, A. Burk-Herrick, M. Westerman, N. A. Ayoub, M. S. Springer, W. J. Murphy, Impacts of the Cretaceous terrestrial revolution and KPg extinction on mammal diversification. *Science* **334**, 521–524 (2011).
24. D. Jablonski, Extinction and the spatial dynamics of biodiversity. *Proc. Natl. Acad. Sci. U.S.A.* **105**, 11528–11535 (2008).
25. S. L. Brusatte, R. J. Butler, A. Prieto-Márquez, M. A. Norell, Dinosaur morphological diversity and the end-Cretaceous extinction. *Nat. Commun.* **3**, 804 (2012).
26. J. D. Archibald, What the dinosaur record says about extinction scenarios, in *Volcanism, Impacts, and Mass Extinctions: Causes and Effects*, G. Keller, A. C. Kerr, Eds. (Geological Society of America, 2014), vol. 505.
27. M. Sakamoto, M. J. Benton, C. Venditti, Dinosaurs in decline tens of millions of years before their final extinction. *Proc. Natl. Acad. Sci. U.S.A.* **113**, 5036–5040 (2016).
28. C. O'Donovan, A. Meade, C. Venditti, Dinosaurs reveal the geographical signature of an evolutionary radiation. *Nat. Ecol. Evol.* **2**, 452–458 (2018).
29. A. A. Chiarenza, P. D. Mannion, D. J. Lunt, A. Farnsworth, L. A. Jones, S.-J. Kelland, P. A. Allison, Ecological niche modelling does not support climatically-driven dinosaur diversity decline before the Cretaceous/Paleogene mass extinction. *Nat. Comm.* **10**, 1091 (2019).
30. C. D. Dean, A. A. Chiarenza, S. C. R. Maidment, Formation binning: A new method for increased temporal resolution in regional studies, applied to the Late Cretaceous dinosaur fossil record of North America. *Paleontology* **63**, 881–901 (2020).
31. F. L. Condamine, G. Guinot, M. J. Benton, P. J. Currie, Dinosaur biodiversity declined well before the asteroid impact, influenced by ecological and environmental pressures. *Nat. Comm.* **12**, 3833 (2021).
32. D. Fraser, L. C. Soul, A. B. Tóth, M. A. Balk, J. T. Eronen, S. Pineda-Munoz, A. B. Shupinski, A. Villaseñor, W. A. Barr, A. K. Behrensmeyer, A. Du, J. T. Faith, N. J. Gotelli, G. R. Graves, A. M. Jukar, C. V. Looy, J. H. Miller, R. Potts, S. K. Lyons, Investigating biotic interactions in deep time. *Trends Ecol. Evol.* **36**, 61–75 (2021).
33. M. J. Lecombe, G. J. Jordan, D. Bryant, S. I. Higgins, The dimensionality of niche space allows bounded and unbounded processes to jointly influence diversification. *Nat. Comm.* **9**, 4258 (2018).
34. J. García-Girón, J. Heino, J. Alahuhta, A. A. Chiarenza, S. L. Brusatte, Palaeontology meets metacommunity ecology: The Maastrichtian dinosaur fossil record of North America as a case study. *Palaeontology* **64**, 335–357 (2021).
35. M. Ohlmann, F. Mazel, L. Chalmrandrier, S. Bec, E. Coissac, L. Gielly, J. Pansu, V. Schilling, P. Taberlet, L. Zinger, J. Chave, W. Thuiller, Mapping the imprint of biotic interactions on β -diversity. *Ecol. Lett.* **21**, 1660–1669 (2018).
36. S. Karasiewicz, S. Dolédec, S. Lefebvre, Within outlying mean indexes: Refining the OMI analysis for the realized niche decomposition. *PeerJ.* **5**, e3364 (2017).
37. J. S. Mitchell, P. D. Roopnarine, K. D. Angielczyk, Late Cretaceous restructuring of terrestrial communities facilitated the end-Cretaceous mass extinction in North America. *Proc. Natl. Acad. Sci. U.S.A.* **109**, 18857–18861 (2012).
38. P. D. Roopnarine, K. D. Angielczyk, Community stability and selective extinction during the Permian-Triassic mass extinction. *Science* **350**, 90–93 (2015).
39. A. D. Muscente, A. Prabh, H. Zhong, A. Eleish, M. B. Meyer, P. Fox, R. M. Hazen, A. H. Knoll, Quantifying ecological impacts of mass extinctions with network analysis of fossil communities. *Proc. Natl. Acad. Sci. U.S.A.* **115**, 5217–5222 (2018).
40. E. E. Saupe, A. Farnsworth, D. J. Lunt, N. Sagoo, K. V. Pham, D. J. Field, Climatic shifts drove major contractions in avian latitudinal distributions throughout the Cenozoic. *Proc. Natl. Acad. Sci. U.S.A.* **116**, 12895–12900 (2019).
41. J. D. Gardner, D. G. DeMar Jr., Mesozoic and Palaeocene lissamphibian assemblages of North America: A comprehensive review. *Palaeobiodivers. Palaeoenvir.* **93**, 459–515 (2013).
42. J. Friedman, T. Hastie, R. Tibshirani, Sparse inverse covariance estimation with the graphical lasso. *Biostatistics* **9**, 432–441 (2008).
43. R. Mazumder, T. Hastie, The Graphical Lasso: New insights and alternatives. *Electron. J. Stat.* **6**, 2125–2149 (2012).
44. D. J. Lunt, A. Farnsworth, C. Loptson, G. L. Foster, P. Markwick, C. L. O'Brien, R. D. Pancost, S. A. Robinson, N. Wrobel, Palaeogeographic controls on climate and proxy interpretation. *Clim. Past* **12**, 1181–1198 (2016).
45. P. J. Valdes, E. Armstrong, M. P. S. Badger, C. D. Bradshaw, F. Bragg, M. Crucifix, T. Davies-Barnard, J. J. Day, A. Farnsworth, C. Gordon, P. O. Hopcroft, A. T. Kennedy, N. S. Lord, D. J. Lunt, A. Marzocchi, L. M. Parry, V. Pope, W. H. G. Roberts, E. J. Stone, G. J. L. Tourte, J. H. T. Williams, The BRIDGE HadCM3 family of climate models: HadCM3@Bristol v1.0. *Geosci. Model Dev.* **10**, 3715–3743 (2017).
46. C. Scotese, N. Wright, PALEOMAP paleodigital elevation models (PaleoDEMs) for the Phanerozoic. www.earthbyte.org/ (2018).
47. S. Dolédec, D. Chessel, C. Gimaret-Carpentier, Niche separation in community analysis: A new method. *Ecology* **81**, 2914–2927 (2000).
48. P. D. Roopnarine, Extinction cascades and catastrophe in ancient food webs. *Paleobiology* **32**, 1–19 (2006).
49. P. Roopnarine, Networks, extinction and paleocommunity food webs. *Nat. Prec.* **10.1038/npre.2010.4433.2** (2010).
50. K. P. Murphy, *Machine Learning: A Probabilistic Perspective* (MIT Press, 2012).
51. P. Bonacich, Power and centrality: A family of measures. *Am. J. Sociol.* **92**, 1170–1182 (1987).
52. C. F. Dormann, M. Bobrowski, D. M. Dehling, D. J. Harris, F. Hartig, H. Lischke, M. D. Moretti, J. Pagel, S. Pinkert, M. Schleuning, S. I. Schmidt, C. S. Sheppard, M. J. Steinbauer, D. Zeuss, C. Kraan, Biotic interactions in species distribution modelling: 10 questions to guide interpretation and avoid false conclusions. *Glob. Ecol. Biogeogr.* **27**, 1004–1016 (2018).
53. C. M. Brown, D. C. Evans, N. E. Campione, L. J. O'Brien, D. A. Eberth, Evidence for taphonomic size bias in the Dinosaur Park Formation (Campanian, Alberta), a model Mesozoic terrestrial alluvial-paralic system. *Palaeogeogr. Palaeoclimatol. Palaeoecol.* **372**, 108–122 (2013).
54. C. M. Brown, N. E. Campione, G. P. Wilson Mantilla, D. C. Evans, Size-driven preservational and macroecological biases in the latest Maastrichtian terrestrial vertebrate assemblages of North America. *Paleobiology* **48**, 210–238 (2022).
55. J. A. Bonser, P. M. Barrett, T. J. Raven, N. Cooper, Dinosaur diversification rates were not in decline prior to the K-Pg boundary. *R. Soc. Open Sci.* **7**, 201195, 2020
56. J. Hummel, M. Clauss, Megaherbivores as pacemakers of carnivore diversity and biomass: Distributing or sinking trophic energy. *Evol. Ecol. Res.* **10**, 925–930 (2008).
57. P. M. Barrett, Paleobiology of herbivorous dinosaurs. *Annu. Rev. Earth Planet. Sci.* **42**, 207–230 (2014).

58. O. Hyvärinen, M. Te Beest, E. le Roux, G. Kerley, E. de Groot, R. Vinita, J. P. G. M. Crowsigt, Megaherbivore impacts on ecosystem and Earth system functioning: The current state of the science. *Ecography* **44**, 1579–1594 (2021).
59. W. J. Ripple, T. M. Newsome, C. Wolf, R. Dirzo, K. T. Everatt, M. Galetti, M. W. Hayward, G. I. H. Kerley, T. Levi, P. A. Lindsey, D. W. Macdonald, Y. Malhi, L. W. Painter, C. J. Sandom, J. Terborgh, B. Van Valkenburgh, Collapse of the world's largest herbivores. *Sci. Adv.* **1**, e1400103 (2015).
60. D. W. Larson, C. M. Brown, D. C. Evans, Dental disparity and ecological stability in bird-like dinosaurs prior to the end-Cretaceous mass extinction. *Curr. Biol.* **26**, 1325–1333 (2016).
61. J. A. MacLaren, P. S. L. Anderson, P. M. Barrett, E. J. Rayfield, Herbivorous dinosaur jaw disparity and its relationship to extrinsic evolutionary drivers. *Paleobiology* **43**, 15–33 (2017).
62. K. K. Nordén, T. L. Stubbs, A. Prieto-Márquez, M. J. Benton, Multifaceted disparity approach reveals dinosaur herbivory flourished before the end-Cretaceous mass extinction. *Paleobiology* **44**, 620–637 (2018).
63. T. R. Lyson, N. R. Longrich, Spatial niche partitioning in dinosaurs from the latest cretaceous (Maastrichtian) of North America. *Proc. Biol. Sci.* **278**, 1158–1164 (2011).
64. J. C. Mallon, D. C. Evans, M. J. Ryan, J. S. Anderson, Feeding height stratification among the herbivorous dinosaurs from the Dinosaur Park Formation (upper Campanian) of Alberta, Canada. *BMC Ecol.* **13**, 14 (2013).
65. A. A. Chiarenza, P. D. Mannion, A. Farnsworth, M. T. Carrano, S. Varela, Climatic constraints on the biogeographic history of Mesozoic dinosaurs. *Curr. Biol.* **32**, 570–585.e3 (2022).
66. G. P. Wilson, Mammalian extinction, survival, and recovery dynamics across the Cretaceous–Paleogene boundary in northeastern Montana, USA, in *Through the End of the Cretaceous in the Type Locality of the Hell Creek Formation in Montana and Adjacent Areas*, G. P. Wilson, W. A. Clemens, J. R. Horner, J. H. Hartman, Eds. (Geological Society of America, 2014), vol. 503.
67. N. R. Longrich, P. J. Currie, *Albertonykus borealis*, a new alvarezsaur (Dinosauria: Theropoda) from the early Maastrichtian of Alberta, Canada: Implications for the systematics and ecology of the Alvarezsauridae. *Cretac. Res.* **30**, 239–252 (2009).
68. D. M. Grossnickle, E. Newham, Therian mammals experience an ecomorphological radiation during the Late Cretaceous and selective extinction at the K–Pg boundary. *Proc. R. Soc. B* **283**, 20160256 (2016).
69. D. J. Field, A. Bercovici, J. S. Berv, R. Dunn, D. E. Fastovsky, T. R. Lyson, V. Vajda, J. A. Gauthier, Early evolution of modern birds dstructured by global forest collapse at the end-Cretaceous mass extinction. *Curr. Biol.* **28**, 1825–1831.e2 (2018).
70. G. M. Erickson, D. K. Zelenitsky, D. I. Kay, M. A. Norell, Dinosaur incubation periods directly determined from growth-line counts in embryonic teeth show reptilian-grade development. *Proc. Natl. Acad. Sci. U.S.A.* **114**, 540–545 (2017).
71. S. A. Walsh, P. M. Barrett, A. C. Milner, G. Manley, L. M. Witmer, Inner ear anatomy is a proxy for deducing auditory capability and behaviour in reptiles and birds. *Proc. Biol. Sci.* **276**, 1355–1360 (2009).
72. G. P. Wilson, A. R. Evans, I. J. Corfe, P. D. Smits, M. Fortelius, J. Jernvall, Adaptive radiation of multituberculate mammals before the extinction of dinosaurs. *Nature* **483**, 457–460 (2012).
73. M. Chen, C. A. E. Strömberg Caroline, G. P. Wilson, Assembly of modern mammal community structure driven by Late Cretaceous dental evolution, rise of flowering plants, and dinosaur demise. *Proc. Natl. Acad. Sci. U.S.A.* **116**, 9931–9940 (2019).
74. N. Brocklehurst, E. Panciroli, G. L. Benevento, R. B. J. Benson, Mammaliaform extinctions as a driver of the morphological radiation of Cenozoic mammals. *Curr. Biol.* **31**, 2955–2963.e4 (2021).
75. T. E. Williamson, S. L. Brusatte, G. P. Wilson, The origin and early evolution of metatherian mammals: The Cretaceous record. *ZooKeys* **465**, 1–76 (2014).
76. T. R. Simões, O. Vernygora, M. W. Caldwell, S. E. Pierce, Megaevolutionary dynamics and the timing of evolutionary innovation in reptiles. *Nat. Comm.* **11**, 3322 (2020).
77. T. L. Stubbs, S. E. Pierce, A. Elsler, P. S. L. Anderson, E. J. Rayfield, M. J. Benton, Ecological opportunity and the rise and fall of crocodylomorph evolutionary innovation. *Proc. R. Soc. B: Biol. Sci.* **288**, 20210069 (2021).
78. K. M. Melstrom, R. B. Irmis, Repeated evolution of herbivorous crocodyliforms during the age of dinosaurs. *Curr. Biol.* **29**, 2389–2395.e3 (2019).
79. J. D. Archibald, L. J. Bryant, Differential Cretaceous/Tertiary extinctions of nonmarine vertebrates; Evidence from northeastern Montana, in *Global Catastrophes in Earth History: An Interdisciplinary Conference on Impacts, Volcanism, and Mass Mortality*, V. L. Sharpton, P. D. Ward, Eds. (Geological Society of America, 1990), vol. 247.
80. P. M. Sheehan, D. E. Fastovsky, Major extinctions of land-dwelling vertebrates at the Cretaceous–Tertiary boundary, eastern Montana. *Geology* **20**, 556–560 (1992).
81. T. R. Lyson, A. Bercovici, S. G. B. Chester, E. J. Sargis, D. Pearson, W. G. Joyce, Dinosaur extinction: Closing the '3 m gap'. *Biol. Lett.* **7**, 925–928 (2011).
82. P. A. Holroyd, G. P. Wilson, J. H. Hutchison, Temporal changes within the latest Cretaceous and early Paleogene turtle faunas of northeastern Montana, in *Through the End of the Cretaceous in the Type Locality of the Hell Creek Formation in Montana and Adjacent Areas*, G. P. Wilson, W. A. Clemens, J. R. Horner, J. H. Hartman, Eds. (Geological Society of America, 2014), vol. 503.
83. B. M. Wynn, D. G. DeMar Jr., G. P. Wilson, Euselachian diversity through the uppermost Cretaceous Hell Creek Formation of Garfield County, Montana, USA, with implications for the Cretaceous–Paleogene mass extinction in freshwater environments. *Cretac. Res.* **13**, 104483 (2020).
84. N. MacLeod, P. F. Rawson, P. L. Forey, F. T. Banner, M. K. Boudagher-Fadel, P. R. Bown, J. A. Burnett, P. Chambers, S. Culver, S. E. Evans, C. Jeffery, M. A. Kaminski, A. R. Lord, A. C. Milner, A. R. Milner, N. Morris, E. Owen, B. R. Rosen, A. B. Smith, P. D. Taylor, E. Urquhart, J. R. Young, The Cretaceous–Tertiary biotic transition. *J. Geol. Soc.* **154**, 265–292 (1997).
85. S. A. Price, L. Schmitz, C. E. Oufiero, R. I. Eytan, A. Dornburg, W. L. Smith, M. Friedman, T. J. Near, P. C. Wainwright, Two waves of colonization straddling the K–Pg boundary formed the modern reef fish fauna. *Proc. Biol. Sci.* **281**, 20140321 (2014).
86. E. C. Sibert, R. D. Norris, New age of fishes initiated by the Cretaceous–Paleogene mass extinction. *Proc. Natl. Acad. Sci. U.S.A.* **112**, 8537–8542 (2015).
87. D. B. Brinkman, J. D. Divay, D. G. DeMar Jr., G. P. Wilson Mantilla, A systematic reappraisal and quantitative study of the nonmarine teleost fishes from the late Maastrichtian of the Western Interior of North America: Evidence from vertebrate microfossil localities. *Can. J. Earth Sci.* **58**, 936–967 (2021).
88. C. A. Brochu, D. C. Parris, B. S. Grandstaff, R. K. Denton, W. B. Gallagher, A new species of *Borealosuchus* (Crocodyliformes, Eusuchia) from the late Cretaceous–early Paleogene of New Jersey. *J. Vertebr. Paleontol.* **32**, 105–116 (2012).
89. D. E. Fastovsky, A. Bercovici, The Hell Creek Formation and its contribution to the Cretaceous–Paleogene extinction: A short primer. *Cretac. Res.* **57**, 368–390 (2016).
90. J. Brugger, G. Feulner, S. Petri, Baby, it's cold outside: Climate model simulations of the effects of the asteroid impact at the end of the Cretaceous. *Geophys. Res. Lett.* **44**, 419–427 (2017).
91. P. M. Barrett, A. J. McGowan, V. Page, Dinosaur diversity and the rock record. *Proc. Biol. Sci.* **276**, 2667–2674 (2009).
92. P. D. Mannion, P. Upchurch, M. T. Carrano, P. M. Barrett, Testing the effect of the rock record on diversity: A multidisciplinary approach to elucidating the generic richness of sauropodomorph dinosaurs through time. *Biol. Rev.* **86**, 157–181 (2011).
93. D. W. Fowler, Revised geochronology, correlation, and dinosaur stratigraphic ranges of the Santonian–Maastrichtian (Late Cretaceous) formations of the Western Interior of North America. *PLOS ONE* **12**, e0188426 (2017).
94. D. Fowler, The Hell Creek Formation, Montana: A stratigraphic review and revision based on a sequence stratigraphic approach. *Geosciences* **10**, 435 (2020).
95. N. Loeuille, M. Loreau, Evolution of body size in food webs: Does the energetic equivalence rule hold? *Ecol. Lett.* **9**, 171–178 (2006).
96. K. Roy, Dynamics of body size evolution. *Science* **321**, 1451–1452 (2008).
97. R. B. J. Benson, Dinosaur macroevolution and macroecology. *Annu. Rev. Ecol. Evol. Syst.* **49**, 379–408 (2018).
98. N. M. Morales-García, P. G. Gill, C. M. Janis, E. J. Rayfield, Jaw shape and mechanical advantage are indicative of diet in Mesozoic mammals. *Commun. Biol.* **4**, 242 (2021).
99. J. García-Girón, J. Heino, F. García-Criado, C. Fernández-Aláez, J. Alahuhta, Biotic interactions hold the key to understanding metacommunity organisation. *Ecography* **43**, 1180–1190 (2020).
100. R. Tibshirani, Regression shrinkage and selection via the Lasso. *J. R. Stat. Soc.* **58**, 267–288 (1996).
101. P. Legendre, L. Legendre, *Numerical Ecology* (Elsevier, 2012).
102. P. Cardoso, F. Rigal, J. C. Carvalho, BAT—Biodiversity assessment tools, an R package for the measurement and estimation of alpha and beta taxon, phylogenetic and functional diversity. *Methods Ecol. Evol.* **6**, 232–236 (2015).
103. R. Foygel, M. Drton, Extended Bayesian information criteria for gaussian graphical models. *Adv. Neural. Inform. Process. Syst.* **23**, 604–612 (2010).
104. S. Epskamp, A. O. J. Cramer, L. J. Waldorp, V. D. Schmittmann, D. Borsboom, qgraph: Network visualizations of relationships in psychometric data. *J. Stat. Soft.* **48**, 1–18 (2012).
105. F. M. Lansac-Tôha, B. A. Quirino, Y. R. Souza, F. A. Lansac-Tôha, L. F. M. Velho, M. T. Baumgartner, The commonality of core biological groups across freshwater food webs. *Limnol. Oceanogr.* **66**, 1459–1474 (2021).
106. A. M. Dunhill, B. Hannisdal, M. J. Benton, Disentangling rock record bias and common-cause from redundancy in the British fossil record. *Nat. Comm.* **5**, 4818 (2014).
107. N. Morueta-Holme, B. Blonder, B. Sandel, B. J. McGill, R. K. Peet, J. E. Ott, C. Violle, B. J. Enquist, P. M. Jørgensen, J.-C. Svenning, A network approach for inferring species associations from co-occurrence data. *Ecography* **39**, 1139–1150 (2016).

108. G. T. Lloyd, A refined modelling approach to assess the influence of sampling on palaeobiodiversity curves: New support for declining Cretaceous dinosaur richness. *Biol. Lett.* **8**, 123–126 (2012).
109. R. J. Butler, R. B. J. Benson, M. T. Carrano, P. D. Mannion, P. Upchurch, Sea level, dinosaur diversity and sampling biases: Investigating the ‘common cause’ hypothesis in the terrestrial realm. *Proc. R. Soc. B* **278**, 1165–1170 (2011).
110. P. D. Mannion, R. B. J. Benson, P. Upchurch, R. J. Butler, M. T. Carrano, P. M. Barrett, A temperate palaeodiversity peak in Mesozoic dinosaurs and evidence for Late Cretaceous geographical partitioning. *Glob. Ecol. Biogeogr.* **21**, 898–908 (2012).
111. M. J. Benton, A. M. Dunhill, G. T. Lloyd, F. G. Marx, Assessing the quality of the fossil record: Insights from vertebrates, in *Comparing the Geological and Fossil Records: Implications for Biodiversity Studies*, A. J. McGowan, A. B. Smith, Eds. (Geological Society of London, 2011), vol. 358.
112. N. Brocklehurst, C. F. Kammerer, J. Fröbisch, The early evolution of synapsids, and the influence of sampling on their fossil record. *Paleobiology* **39**, 470–490 (2013).
113. L. Duarte, P. Prieto, V. Pillar, Assessing spatial and environmental drivers of phylogenetic structure in Brazilian *Araucaria* forests. *Ecography* **35**, 952–960 (2012).
114. M. M. Gossner, T. M. Lewinsohn, T. Kahl, F. Grassein, S. Boch, D. Prati, K. Birkhofer, S. C. Renner, J. Sikorski, T. Wubet, H. Arndt, V. Baumgartner, S. Blaser, N. Blüthgen, C. Börschig, F. Buscot, T. Diekötter, L. R. Jorge, K. Jung, A. C. Keyel, A.-M. Klein, S. Klemmer, J. Krauss, M. Lange, J. Müller, J. Overmann, E. Pašalić, C. Penone, D. J. Perović, O. Purschke, P. Schall, S. A. Socher, I. Sonnemann, M. Tschapka, T. Scharmtke, M. Türke, P. C. Venter, C. N. Weiner, M. Werner, V. Wolters, S. Wurst, C. Westphal, M. Fischer, W. W. Weisser, E. Allan, Land-use intensification causes multitrophic homogenization of grassland communities. *Nature* **540**, 266–269 (2016).
115. W. Atmar, B. D. Patterson, The measure of order and disorder in the distribution of species in fragmented habitat. *Oecologia* **96**, 373–382 (1993).
116. J. C. Carvalho, P. Cardoso, P. A. V. Borges, D. Schmera, J. Podani, Measuring fractions of beta diversity and their relationships to nestedness: A theoretical and empirical comparison of novel approaches. *Oikos* **122**, 825–834 (2013).
117. S. Holm, A simple sequentially rejective multiple test procedure. *Scand. Stat. Theory Appl.* **6**, 65–70 (1979).
118. M. Kuhn, K. Johnson, Remedies for severe class imbalance, in *Applied Predictive Modeling*, M. Kuhn, K. Johnson, Eds. (Springer, 2013), pp. 419–443.
119. M. Kuhn, K. Johnson, Data pre-processing, in *Applied Predictive Modeling*, M. Kuhn, K. Johnson, Eds. (Springer, 2013), pp. 27–59.
120. A. Ross, V. L. Willson, Paired samples T-test, in *Basic and Advanced Statistical Tests: Writing Results Sections and Creating Tables and Figures*, A. Ross, V. L. Willson, Eds. (SensePublishers, 2017), pp. 17–19.
121. A. Farnsworth, D. J. Lunt, C. L. O’Brien, G. L. Foster, G. N. Inglis, P. Markwick, R. D. Pancost, S. A. Robinson, Climate sensitivity on geological timescales controlled by nonlinear feedbacks and ocean circulation. *Geophys. Res. Lett.* **46**, 9880–9889 (2019).
122. A. A. Chiarenza, thesis, Imperial College London (2019).
123. E. M. Dunne, A. Farnsworth, S. E. Greene, D. J. Lunt, R. J. Butler, Climatic drivers of latitudinal variation in Late Triassic tetrapod diversity. *Palaeontology* **64**, 101–117 (2021).
124. A. M. Waterson, D. N. Schmidt, P. J. Valdes, P. A. Holroyd, D. B. Nicholson, A. Farnsworth, P. M. Barrett, Modelling the climatic niche of turtles: A deep-time perspective. *Proc. Biol. Sci.* **283**, 20161408 (2016).
125. G. L. Foster, D. L. Royer, D. J. Lunt, Future climate forcing potentially without precedent in the last 420 million years. *Nat. Commun.* **8**, 14845 (2017).
126. G. E. Hutchinson, Concluding Remarks. *Cold Spring Harb. Symp. Quant. Biol.* **22**, 415–427 (1957).
127. E. Tales, P. Keith, T. Oberdorff, Density-range size relationships in French riverine fishes. *Oecologia* **138**, 360–370 (2004).
128. J. Heino, M. Grönroos, Untangling the relationships among regional occupancy, species traits, and niche characteristics in stream invertebrates. *Ecol. Evol.* **4**, 1931–1942 (2014).
129. J. Heino, K. T. Tolonen, Ecological niche features override biological traits and taxonomic relatedness as predictors of occupancy and abundance in lake littoral macroinvertebrates. *Ecography* **41**, 2092–2103 (2018).
130. S. Dray, A.-B. Dufour, The ade4 package: Implementing the duality diagram for ecologists. *J. Stat. Soft.* **22**, 1–20 (2007).
131. O. J. Dunn, Multiple comparisons using rank sums. *Dent. Tech.* **6**, 241–252 (1964).
132. R Core Team, R: A language and environment for statistical computing, www.R-project.org/ (2020).
133. M. J. Vavrek, H. C. E. Larsson, Low beta diversity of Maastrichtian dinosaurs of North America. *Proc. Natl. Acad. Sci. U.S.A.* **107**, 8265–8268 (2010).

Acknowledgments

Funding: Academy of Finland supported J.G.-G., J.H. (grant no. 331957), and J.A. (grant no. 322652). J.G.-G.’s contribution was also funded by the European Union Next Generation EU/PRTR (grant no. AG325). S.L.B. and A.A.C. were supported through a European Research Council (ERC) Starting Grant under the European Union’s Horizon 2020 Research and Innovation Programme (grant nos. 756226 and 947921, respectively). A.A.C. was also funded through a Juan de la Cierva Formación 2020 Fellowship funded by the Ministry of Science and Innovation from the European Union Next Generation EU/PRTR. D.G.D. and G.P.W.M. were supported by the David B. Jones Foundation and the Myhrvold and Havranek Charitable Family Fund. P.D.M.’s contribution was funded through a Royal Society University Research Fellowship (grant no. UF160216) and a Leverhulme Trust Research Project Grant (grant no. RPG-2021-202). T.E.W. and S.L.B. were also supported by the National Science Foundation (grant nos. EAR 1325544 and DEB 1654952). Silhouettes and pictures used throughout this paper are from <http://phylopic.org/> and Wikimedia Commons courtesy of A. Farke (under CC BY 3.0, <https://creativecommons.org/licenses/by/3.0/>), Ballista (under CC BY-SA 3.0, <https://creativecommons.org/licenses/by-sa/3.0/>), C. Brown (under CC BY-SA 3.0, <https://creativecommons.org/licenses/by-sa/3.0/>), the Children’s Museum of Indianapolis (under CC BY-SA 3.0, <https://creativecommons.org/licenses/by-sa/3.0/>), Durbed (under CC BY-SA 3.0, <https://creativecommons.org/licenses/by-sa/3.0/>), F. Wierum (under CC BY-SA 4.0, <https://creativecommons.org/licenses/by-sa/4.0/>), J. Headden (under CC BY-NC-SA 3.0, <https://creativecommons.org/licenses/by-nc-sa/3.0/>), L. Weaver (modified after artwork by M. Ouchida, under CC BY 3.0, <https://creativecommons.org/licenses/by/3.0/>), M0tty (under CC BY-SA 3.0, <https://creativecommons.org/licenses/by-sa/3.0/>), N. Tamura (under CC BY-SA 3.0, <https://creativecommons.org/licenses/by-sa/3.0/>), Rama (under CC BY-SA 3.0, <https://creativecommons.org/licenses/by-sa/3.0/>), R. Díaz Sibaja (under CC BY 3.0, <https://creativecommons.org/licenses/by-nc-sa/3.0/>), T. M. Keeseey (under CC BY-SA 3.0, <https://creativecommons.org/licenses/by-sa/3.0/>), W. Vladimir (under CC BY 3.0, <https://creativecommons.org/licenses/by/3.0/>), Z. Evenor (under CC BY 3.0, <https://creativecommons.org/licenses/by/3.0/>), and Zimices (under CC BY 3.0, <https://creativecommons.org/licenses/by/3.0/>). This is Paleobiology Database official publication number 435. **Author contributions:** Conceptualization: J.G.-G., A.A.C., J.A., J.H., and S.L.B. Methodology: J.G.-G., J.A., and J.H. Investigation: J.G.-G., A.A.C., D.G.D., P.D.M., T.E.W., G.P.W.M., and S.L.B. Visualization: J.G.-G. Supervision: J.G.-G., A.A.C., and S.L.B. Writing—original draft: J.G.-G., A.A.C., and S.L.B. Writing—review and editing: All authors. **Competing interests:** The authors declare that they have no competing interests. **Data and materials availability:** List of statistical routines (data S1) and cleaned fossil datasets from the Paleobiology Database (data S2 and S3) are available on Zenodo (<https://doi.org/10.5281/zenodo.7221223>). Earth System models and paleoenvironmental envelopes are freely available using citations in the manuscript. All data needed to evaluate the conclusions in the paper are present in the paper and/or the Supplementary Materials.

Submitted 15 June 2022

Accepted 4 November 2022

Published 7 December 2022

10.1126/sciadv.add5040